JOURNAL OF CATALYSIS 81, 107–118 (1983)

The Characterisation of a Model Platinum/Alumina Catalyst by High-Resolution Electron Microscopy

DAVID J. SMITH

High Resolution Electron Microscope, University of Cambridge, Free School Lane, Cambridge CB2 3RQ, England

AND

D. WHITE,* T. BAIRD, AND J. R. FRYER

Chemistry Department, University of Glasgow, Glasgow G12 8QQ, Scotland

Received August 5, 1982

Model catalysts consisting of platinum particles on a thin alumina support were examined by electron microscopy following various oxidative and reducing treatments. Details of particle size distributions were obtained and particle sintering was shown to depend on treatment temperature, atmosphere, and metal loading, being greatest in a "chlorided" oxygen environment and least in a *pure* hydrogen one. Trace impurities, even at the 1-vpm level, were shown to enhance significantly the sintering rate in a reducing atmosphere. High-resolution observations at the direct lattice imaging level provided information about both particle and support morphology, in particular establishing that most particles consist substantially of metallic platinum, either in single-crystal form or often twinned. The relevance of model catalyst studies to "real" catalysts is briefly discussed.

1. INTRODUCTION

In recent years there has been increasing interest in the structure and properties of simplified model catalyst systems usually consisting of noble metal particles supported on some convenient ceramic support. Particular attention has been directed towards the platinum/alumina system because of its similarity to functional industrial catalysts and the need to account for the phenomena of sintering and re-dispersion in the latter. Model platinum/alumina systems have been used to follow changes in particle structure and morphology as a result of treatments involving different atmospheres and temperatures as well as the influence of the particle support and its method of preparation (*1–10*). It appears that redispersion may be possible following heating in an oxygen-rich atmosphere (*1, 3, 4, 6, 11*), although the experimental conditions and the mechanisms by which this can take place have been disputed (*7, 8*).

A major problem with Pt/alumina catalysts is their general loss of activity, following use at elevated temperatures, which is presumed to be due to a reduction in the surface area available for catalytic exchange. For industrial catalysts, activity has been restored by controlled oxidation to remove carbonaceous residues followed by heating in oxygen/chloride mixtures (*12*). Although the mode of regeneration remains controversial, as mentioned above, an understanding of the regeneration process is crucial to the comprehension of platinum/alumina catalysts since the precise sites of catalytic activity are unknown. One proposed mechanism is that, during the ageing of the catalyst, an increase in particle size (i.e., sintering) takes place thereby reducing the available surface area for a given loading of platinum on the support; the regeneration treatment breaks the large

* Present address: Analytical Services & Research Division, B.P. Research Centre, Chertsey Road, Sunbury-on-Thames, Middlesex TW16 7LN, England.

0021-9517/83 $3.00

particles into smaller ones with consequent increase in activity (e.g., Ref. (*3*)). The formation of a platinum oxide yielding smaller platinum particles on subsequent reduction has also been proposed (e.g., Refs. (*6, 13, 14*)). Alternatively, it could be considered that the primary platinum particle size is irrelevant since it has been suggested (e.g., Ref. (*11*)) that the particles merely act as reservoirs for platinum atoms of a platinum surface complex in the vicinity of the particle where catalysis takes place.

A model system cannot demonstrate the catalytic behavior of a real catalyst because of the much smaller total area of a few particles on a small flat surface compared to the very high surface area of a real catalyst, but it can nevertheless be used to duplicate the behaviour of platinum particles in a local environment provided that this is similar to that of a real catalyst support. In consequence, transmission electron microscopy (TEM) can play a major role in providing information on individual particle behaviour of suitable model catalysts. Note, however, that the use of electron microscopy can introduce concomitant pitfalls. Glassl *et al.* (*9*) have shown that the preparation of samples by chemical stripping can sometimes produce structural changes greater than those arising from the actual catalytic reaction. Thus, precautions were taken in the present work to maintain well-controlled experimental conditions involving a minimum of specimen handling and the elimination of trace impurities during heat treatment (*15, 16*). Moreover, as pointed out elsewhere (*17, 18*), considerable care should be exercised in the interpretation of electron micrographs of small particles, particularly with regard to their orientation, size, and shape, because of the perturbing influences of instrumental aberrations and high support contrast.

This paper describes a model platinum/alumina catalyst subjected to a variety of heat treatments in different gaseous atmospheres. General TEM observations provided statistical information concerning particle sintering and mobility behaviour, whilst direct lattice imaging with the Cambridge University 600-kV high-resolution electron microscope (HREM) (*19, 20*) provided invaluable structural details of the particles and their support. In a companion paper we describe further observations of a functional Pt/alumina reforming catalyst (*21*). Some of the preliminary results of this study have been reported elsewhere (*15, 16*).

2. EXPERIMENTAL

2.1. Preparation of alumina supports. Several techniques were used in preparing films of alumina for use as model catalyst supports which were also thin enough for HREM observations. These were: vacuum evaporation of alumina from various high-melting-point metal filaments; alumina sputtering using a high-energy electron beam source; and preparation of thin aluminium films with subsequent oxidation. Vacuum evaporation of γ-Al_2O_3, as follows, generally proved to be the most suitable.

"Condea" SB Pural Alc 169 hydrated alumina was first calcined at 550°C in air. Some of the calcined material was then placed in a tantalum boat inside a vacuum coating unit and evacuated to better than 4×10^{-5} Torr overnight at room temperature to remove excess adsorbed water. The tantalum boat was then electrically heated to evaporate the alumina onto the clean face of a freshly cleaved rock salt crystal. Film thicknesses ($\leq$200 Å) were measured by a quartz crystal thickness monitor or estimated visually during evaporation.

2.2. Deposition of platinum. Platinum was evaporated onto the resulting alumina films from a resistance-heated tungsten filament. The metal loading was varied either by controlling the amount evaporated or sometimes (when heavier loadings were required) by carrying out two or three evaporations. Note that all direct comparisons of time, temperature, and atmosphere were carried out for identical metal loadings.

Comparisons of different metal loadings are discussed separately below.

2.3. Heat treatments. Freshly prepared model catalysts, with varying Pt-loadings, were subjected to various time, temperature, and atmosphere treatments by placing TEM specimen grids, already loaded with the films, in the hot zone of a furnace. Alternatively, rock salt crystals plus model film could be treated; after cooling down, the NaCl was dissolved in deionised water leaving model films floating on the surface to be picked up on specimen grids for subsequent examination. No effect due to the rock salt was observed. Standard cycles involved overnight flushing with nitrogen or the reactant gas, heating to the required temperature over 30 min, and then maintaining this typically for a further 30 min before slow cooling to room temperature. Variations are noted in Tables 1 to 4. The temperature in the hot zone of the barrel furnace was measured using a chromel–alumel thermocouple and, for more accurate temperature control, further calibration using a Derritron Co thermocouple potentiometer ensured that temperature variation was not more than ±2°C from that recorded.

Flow experiments were carried out in methane, commercial-grade hydrogen, purified hydrogen, wet hydrogen, nitrogen, 3% by volume of oxygen in nitrogen, and "chlorided" 3% O_2/N_2: some static experiments in air or vacuum (using a coating unit) were also performed. The methane, supplied by Matheson Co., was C.P. grade 99% pure. Impure hydrogen was used, as supplied by B.O.C. C.P. grade, containing not more than 1 vpm water, 1 vpm oxygen, and 1 vpm hydrocarbon impurities. For the experiments with pure hydrogen, these impurities were removed by passage through an Engelhard "Deoxo" purifier and liquid nitrogen trap with 4A molecular sieves. B.O.C. oxygen-free nitrogen and Air Products 3% oxygen in nitrogen were dried before use. In experiments with wet hydrogen or "chlorided" oxygen/nitrogen, water and carbon tetrachloride, respectively, were added to the gas flow from a side port, with the vapour pressure of the additive controlled by various hot/cold traps. Added trace impurities were monitored at the exit vent with, and without, the sample in place by means of a Dräger multigas detector. Note that all gas lines and valves were made of stainless steel with grease-free Swagelok couplings; feedline and reaction tube were made from silicon glass with PTFE dryseals. The apparatus was rotary-evacuated periodically to check for leaks.

2.4. Electron microscopy. All characterisations of particle size distributions were carried out with a JEM-100C electron microscope operated at 100 kV, with electron micrographs generally being recorded at magnifications of between 20,000–100,000 times. Detailed high-resolution examination of some samples was subsequently made with the 600-kV HREM (*19, 20*), which had previously demonstrated a directly interpretable resolution approaching 0.2 nm and an ability to resolve lattice fringes finer than 0.1 nm (*21*). Operation of the latter microscope was normally at 500 kV using axial bright-field illumination, with micrographs recorded at magnifications of 200,000–300,000 times. Substrate charging in the electron beam was often a problem at these high magnifications but could be alleviated by mounting the alumina films on holey carbon support films premounted on microscope grids with imaging restricted to the region of the holes.

2.5. Statistical analyses. Particle size distributions (PSDs) for small-diameter particles were measured from photographic enlargements of the original micrographs, whilst direct measurement from the negatives was used for the larger particles; the mean of the longest and shortest diameters was taken for irregularly shaped particles. The normal statistical formulae were used for calculation of the mean diameter d, and the variance on the mean, σ, for counts of n particles, each of diameter d:

$$\bar{d} = \frac{\Sigma d}{n} \quad \text{and} \quad \sigma = \pm \frac{\sqrt{\Sigma(|\bar{d} - d|^2)}}{n}.$$

3. RESULTS

3.1. Particle Size Distributions

Statistical results from some of the heat treatments are summarised in Tables 1 to 4, where it can also be seen that the various means and standard deviations were normally based on samples of 200 counts or more. These analyses aimed at characterising general trends as functions of both time and temperature, as well as establishing the differing effects of the prevailing atmosphere during treatment. Those samples marked (*a*) were later examined in the high-resolution electron microscope. The platinum loading was varied considerably so that direct comparisons between different preparations were not always possible. However, it was significant that, despite the differences in loading, the particle size distributions (PSDs) were initially quite similar (see Fig. 1) except in the case of the heaviest loadings where particle coalescence started to occur. Following heat treatment, substantial differences became apparent; these are described below. More details of particle morphologies are also given in Section 3.4. Finally, it should be noted that the major part of any change in the PSD generally occurred within the first hour of any treatment cycle and there was normally little change of statistical significance after 2 hr (e.g., MC16—Table 1). Consequently, heat treatments were normally restricted to 1 or 2 hr at most.

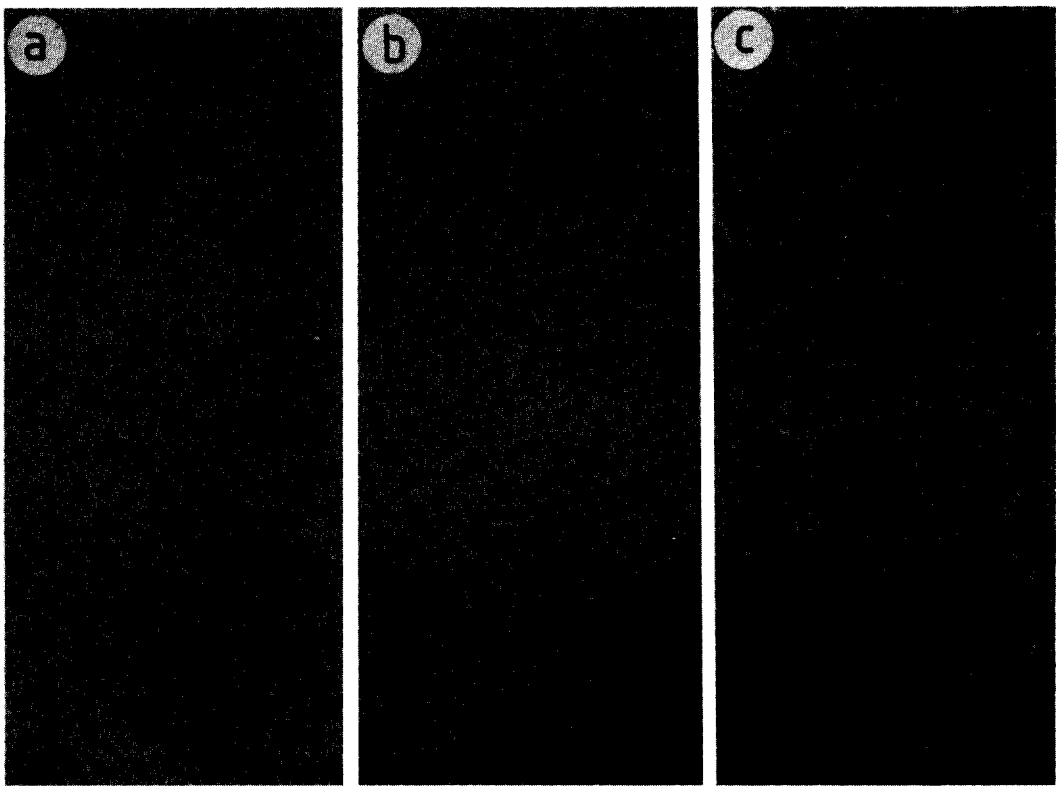

FIG. 1. Low-magnification images of platinum particles supported on thin films of evaporated γ-alumina, showing the different metal loadings. (a) Model catalyst MC14; (b) MC15; (c) MC16.

TABLE 1

Variation of PSD for Model Catalyst MC16 following Treatment Cycles in Chlorided 3 v/o O_2/N_2 Atmosphere at 300°C

Treatment details	$\bar{d}$ (nm)	σ (nm)	No. of counts
0.5 hr	8.5	1.7	200
1.0	8.2	2.0	200
1.5	9.5	2.2	200
2.0	10.2	2.3	200
3.0	10.5	2.0	200
4.5	10.8	2.4	200

TABLE 2

Variation of PSD for Model Catalyst MC14

Treatment details	$\bar{d}$ (nm)	σ (nm)	No. of counts
Fresh	1.8	0.6	520
H_2(pure)/500°C/1 hr	2.1	0.7	306
H_2(impure)/500°C/1 hr	3.8	1.5	82
H_2(wet)/500°C/1 hr	3.0	1.3	134
CH_4/500°C/1 hr	3.2	1.0	138

3.2. Effect of Impurities

It has previously been reported that the methods used for preparing model catalysts in a form suitable for electron microscopy can produce changes substantially greater than those normally produced in subsequent treatment of the model (*9*). Our results for the model catalyst MC14 (see Table 2 and Fig. 2) established that the presence of impurities, albeit in trace form only, could also lead to considerable changes in the PSD. The sample heated in pure hydrogen at 500°C exhibited minimal sintering, increasing in mean diameter from 1.8 to 2.3 nm, whereas those samples treated in wet or "impure" hydrogen increased in particle diameter substantially to 3.0 and 2.8 nm, respectively. It is interesting to compare these changes with the effect of a methane atmosphere where the increase was to 3.2 nm.

3.3. Effect of Temperature

In "oxidising" environments, the effect of increased temperature was to produce

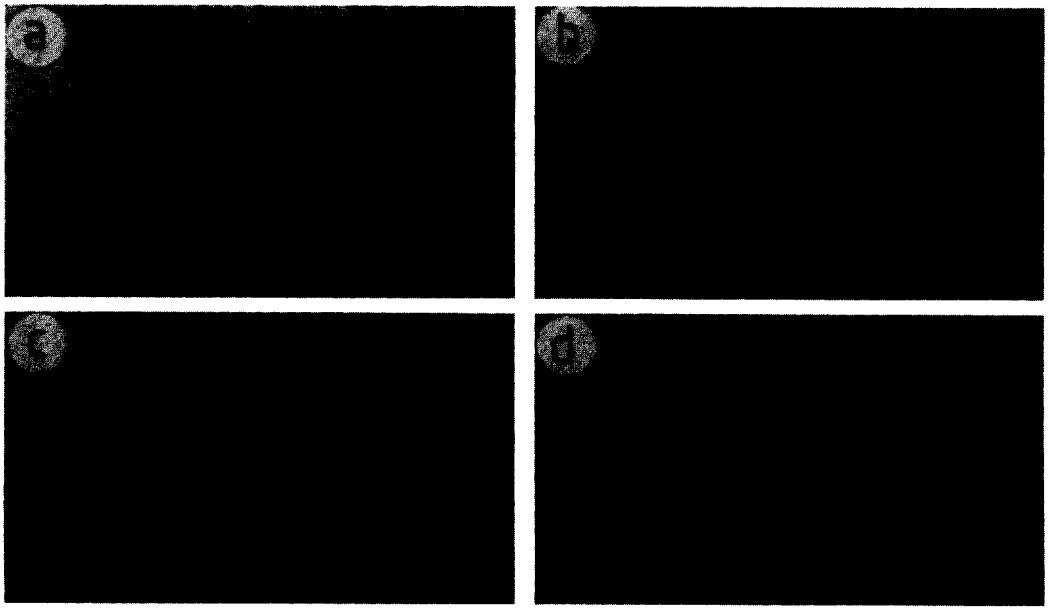

FIG. 2. Model catalyst MC14 after reduction at 500°C for 1 hr showing the influence of various atmospheres and impurities. (a) "Pure" H_2; (b) "wet" H_2; (c) "impure" H_2; (d) methane.

TABLE 3

Variation of PSD for Model Catalyst MC15

Treatment details	$\bar{d}$ (nm)	σ (nm)	No. of counts
H_2(pure)/500°C/1 hr	4.8	1.5	200
3 v/o O_2 in N_2/200°C/1 hr	—	—	—
+ 3 v/o O_2 in N_2/300°C/1 hr	6.1	1.6	200
+ 3 v/o O_2 in N_2/400°C/1 hr	11.2	2.6	200
3 v/o O_2 in N_2/CCl_4/200°C/1 hr	3.4	1.2	2600
+ 3 v/o O_2 in N_2/CCl_4/300°C/1 hr	9.6[a]	1.8	392
+ 3 v/o O_2 in N_2/CCl_4/400°C/1 hr	22.9	4.0	241
+ 3 v/o O_2 in N_2/CCl_4/500°C/1 hr	33.3[a]	5.1	200

[a] Examined also in the high-resolution electron microscope.

TABLE 4

Variation of PSD for Model Catalyst MC20

Treatment details	$\bar{d}$ (nm)	σ (nm)	No. of counts
Fresh	1.8[a]	0.4	186
H_2(pure)/500°C/2 hr	4.0	0.8	145
H_2(pure)/600°C/2 hr	4.1[a]	1.1	252
H_2(pure)/600°C + 500°C/2 hr ea.	4.7	1.2	298
3 v/o O_2 in N_2/500°C/2 hr	25.0	9.0	350
3 v/o O_2 in N_2/600°C/2 hr	43.0[a]	16.7	334
3 v/o O_2 in N_2/600°C + 500°C/2 hr ea.	46.7	12.0	290
3 v/o O_2 in N_2/CCl_4/300°C/1 hr	3.6[a]	0.8	276
3 v/o O_2 in N_2/CCl_4/400°C/1 hr	5.3	0.9	275

[a] Examined also in the high-resolution electron microscope.

substantial particle sintering. This is typified by the two cycles tabulated for the model catalyst MC15 (see Table 3 and Fig. 3), as well as some of the treatments given to MC20 (see Table 4). It is also significant that the influence of "chlorination" is to further enhance the sintering behaviour. For model MC15, for example, it can be seen in Table 3 that the added traces of CCl_4 resulted in a mean diameter of 9.6 nm rather than 6.1 nm, after both samples had been treated for 1 hr at 200°C, followed by 1 hr at 300°C. A further hour's treatment at 400°C led to an even greater difference: 22.9 nm instead of 11.2 nm.

In "reducing" atmospheres, particle sintering was less by comparison and, moreover, increased temperature did not seem to influence very much the amount of sintering; particle rounding then appeared to be the major change. Indeed, when the platinum loading was low, as, for example, in

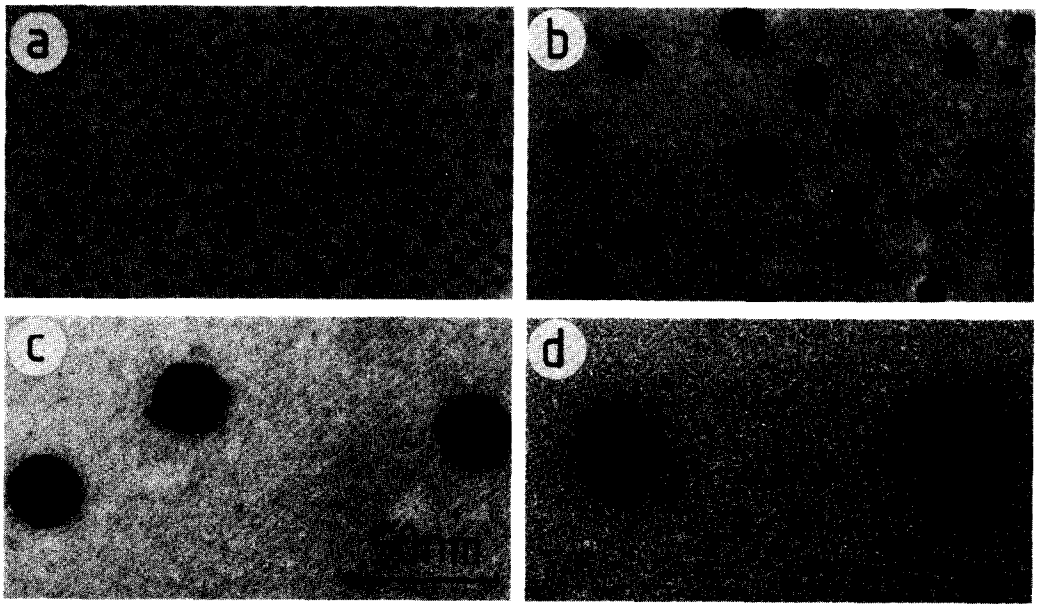

FIG. 3. Changes in model catalyst MC15 after successive treatments in 3% v/v O_2/N_2: (a) At 200°C/1 hr; (b) +300°C/1 hr; (c) +400°C/1 hr; (d) +500°C/1 hr.

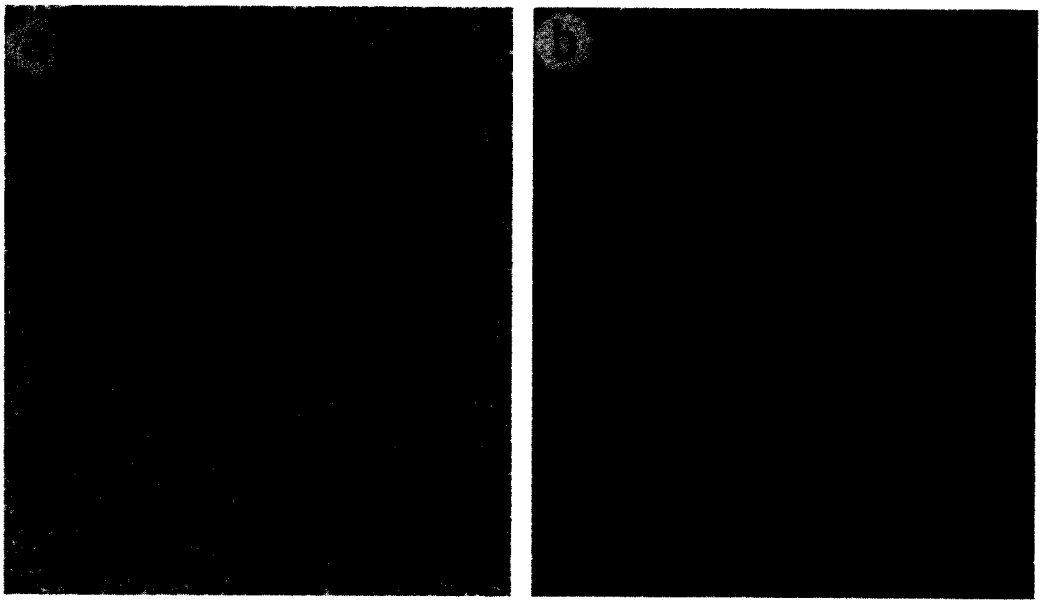

FIG. 4. (a) Model catalyst MC20 when fresh, (b) change produced by heating in hydrogen at 600°C for 2 hr. Note different image magnifications.

MC14 (see Table 2), heating in pure hydrogen at 500°C had minimal effect, increasing the mean particle diameter from 1.8 to only 2.1 nm. When the platinum loading was higher, as, for example, with MC20 (see Table 4), the increase in mean particle diameter was greater, going to 4.0 nm at 500°C. However, effectively the same mean diameter was obtained on heating to 600°C. Figure 4 illustrates the change produced in model catalyst MC20: Fig. 4a shows the sample when fresh and Fig. 4b shows the result of heat treatment in pure hydrogen at 600°C for 2 hr.

3.4. High-Resolution Observations

In all model systems examined, particles consisting of metallic platinum only were observed; these were identified directly from the spacings of the various lattice fringes visible. Overall, the most common structural type observed in the particles was the single crystal, although lamellar twins were relatively common and multiply twinned particles (MTPs) were sometimes observed. The differences in particle morphologies which result from the various heat treatment cycles are illustrated by the following representative samples.

(i) Fresh catalyst (MC 20). This sample, shown at high magnification in Fig. 5, consisted of irregularly shaped particles of platinum, mostly in the approximate size range 0.5–2.0 nm. Lattice fringe structure was visible in many particles with the 0.227-nm (111) and 0.198-nm (200) spacings being most prevalent. It should also be noted that the relative orientations of the particles generally seemed to be quite random and bore no obvious relationship with the structure of the support. The small, polycrystalline nature of the sample was confirmed by electron diffraction patterns which consisted primarily of broad continuous rings, peaked at the Pt-lattice spacings. Many of the particles were covered entirely by only one set of fringes, indicating that they were single crystals, but others had obvious discontinuities where fringes either terminated, or were mirrored at the boundary, which suggested lamellar twinning. The alumina support film generally appeared to be amorphous but micro-domains of γ-Al_2O_3, again confirmed by measurement of

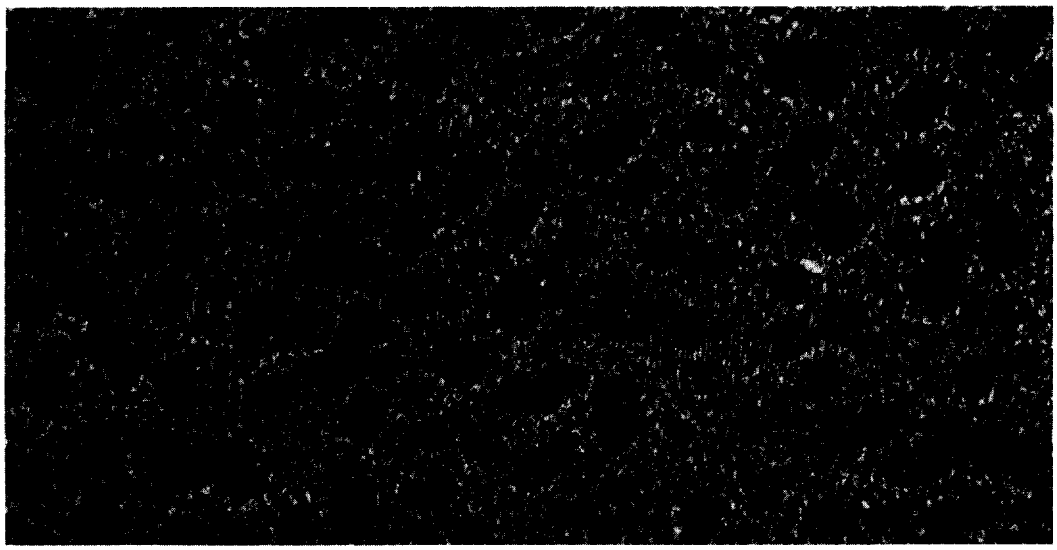

FIG. 5. High-magnification image of MC20 when fresh showing small, irregularly shaped Pt particles of low contrast. Lattice fringes are visible in both the particles and the support.

lattice fringe spacings, were often observed.

(ii) Reduction—H_2 at 600°C (MC 20). This sample (see Fig. 4b) consisted of small particles of platinum distributed in size about a mean of 4.0 nm. Particles generally had a well-rounded appearance with the lattice fringes visible in many of these indicating single crystals or lamellar twins. Microdomains were again visible in the alumina matrix although there was no evidence for substantial changes as a result of heat treatment. Moreover, there was no evidence to suggest any sintering action due to the support.

(ii) Oxidation—O_2/N_2 at 600°C (MC 20). The most striking thing about this sample, apart from the mean particle size, was the large variation in particle morphology, as shown, for example, in Fig. 6a. Twinning seemed to be commonplace and many particles had the appearance of two or more smaller particles simply "fusing" together (see Fig. 6b). Many seemed to have amorphous material, of higher contrast than the support film, extending along faceted edges of the crystals (see Fig. 6c) and many had long straight edges (see Figs. 6a–c). A small number of multiply twinned particles were observed, usually with re-entrant surface structure (see Fig. 6d) at the twin boundaries. Lattice fringes, with spacings again corresponding to metallic platinum, could be seen in many of these particles.

(iv) Oxychlorination—O_2/N_2 with CCl_4 at 300°C (MC 15 and MC 20). The PSDs for these two model catalysts after treatment were considerably different (see Tables 1 and 4) because of the differences in Pt-loading of the original fresh catalysts (see Fig. 1). However, the overall particle morphology in both samples was quite similar: particles were well rounded and crystalline with about 30% visibly twinned. Figure 7a shows a typical region of MC20 at high magnification whilst Fig. 7b shows a striking example of a γ-Al_2O_3 micro-twin. The only apparent difference in these two samples after treatment, other than size, was that some of the larger particles of MC15 exhibited more complicated lamellar twinning; an interesting example is shown in Fig. 7c.

(v) Oxychlorination—O_2/N_2 with CCl_4 at

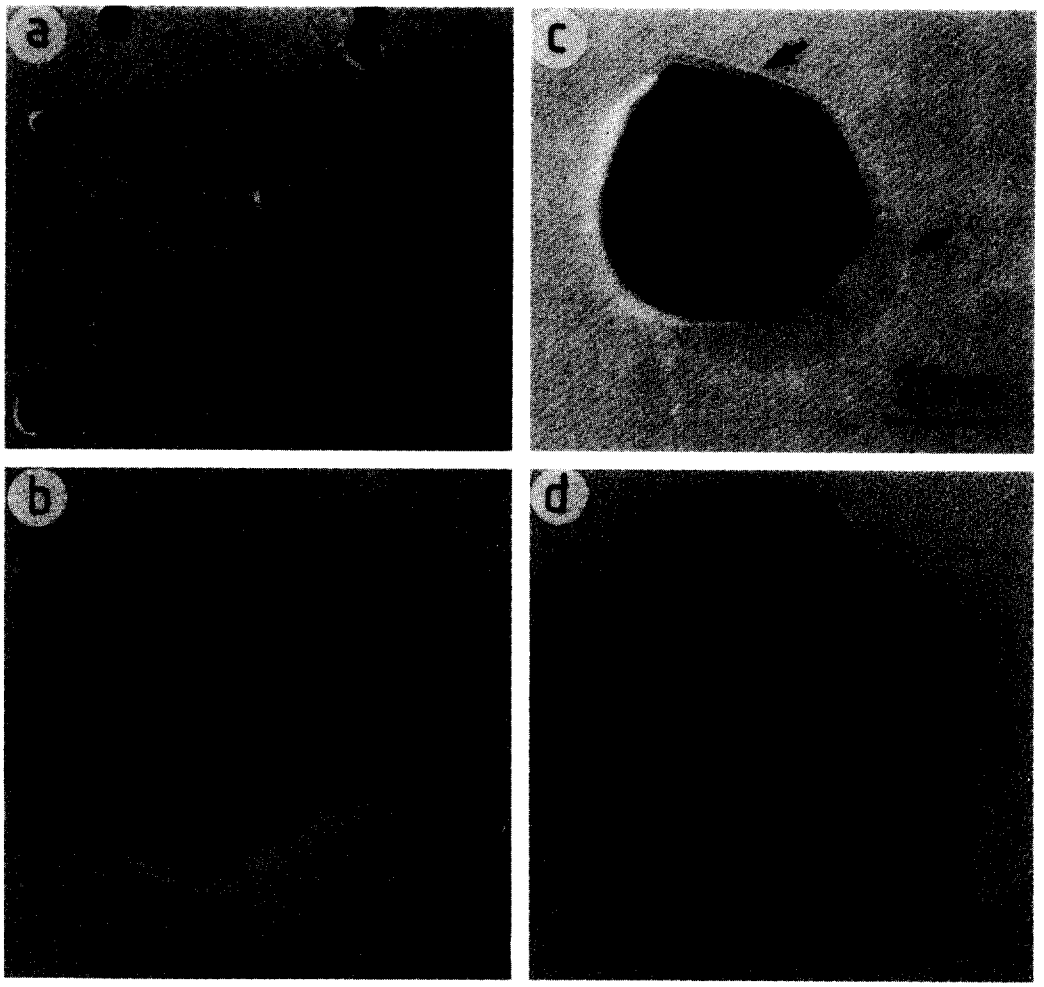

FIG. 6. Various Pt particles seen in MC20 following oxidation at 600°C in 3 v/o O_2/N_2. (a) Low-magnification field of view; (b) two particles apparently "fusing" together; (c) amorphous material (arrowed) on substrate surrounding faceted crystal; (d) multiply twinned particle with re-entrant surface structure (arrowed).

500°C (MC 15). High-resolution observations revealed that the particles present in this sample were generally well rounded and mostly single crystals of platinum, as already found for the same sample heated to 300°C (see (iv)), although the substantial difference in PSDs should be noted. Lamellar twinning was again evident (see Fig. 8a) and some particles appeared to have some sort of amorphous, or poorly crystalline, region surrounding them (see Fig. 8b). There was no obvious change in the texture or crystallinity of the substrate.

4. DISCUSSION

Whilst there are obvious differences between the platinum/alumina model catalysts examined here and "real" catalysts of industrial importance, there are several aspects of the present study which are of relevance to the latter and these are discussed below. The model catalysts generally had a heavy metal loading, thus making particle nearest-neighbour separations quite small and particle growth easier. Moreover, the alumina support of the model does not have

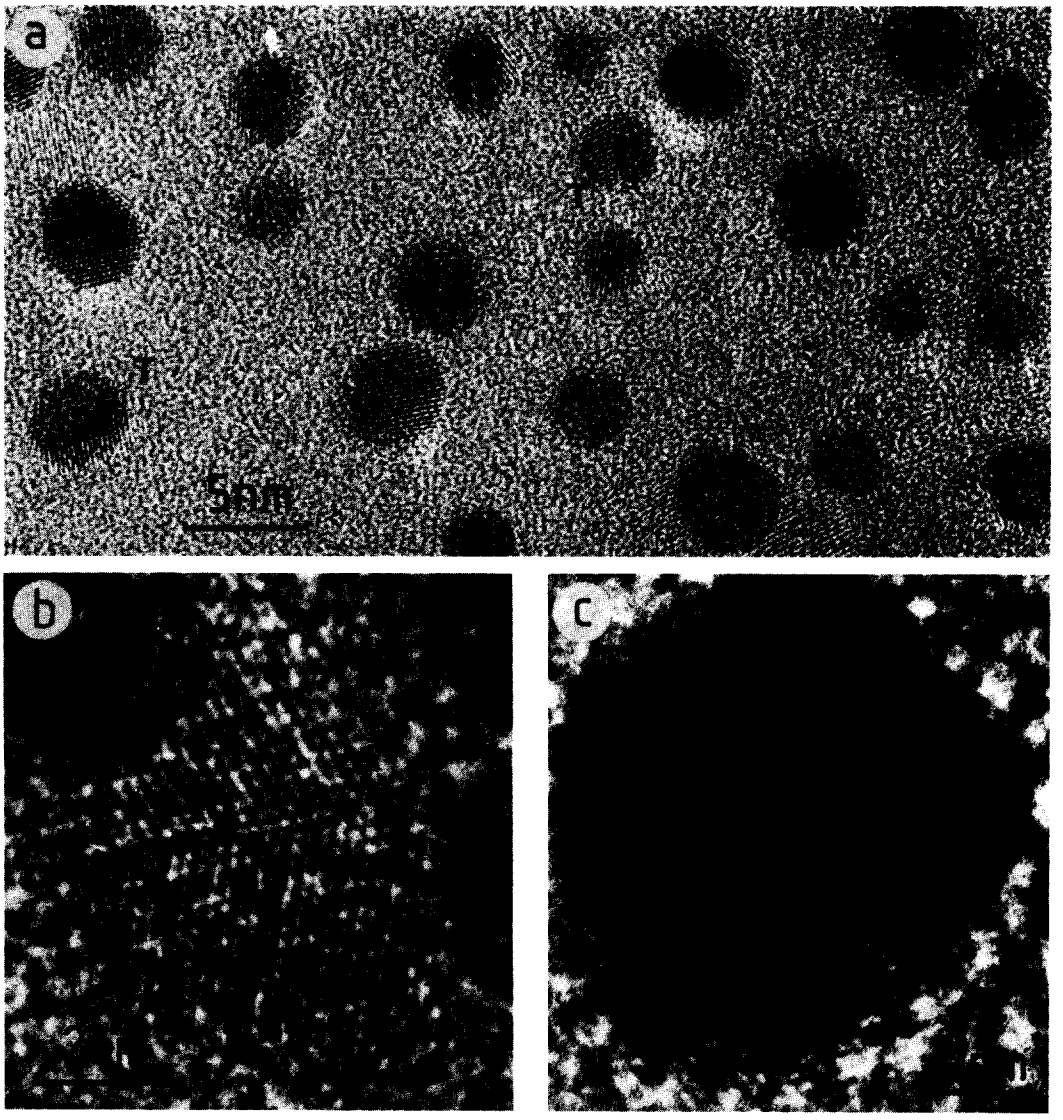

FIG. 7. After "oxychlorination" at 300°C: (a) MC20—note lattice fringes in Pt particles and evidence for twinning (T); (b) micro-twin visible in γ-Al_2O_3 support; (c) MC15—complex twinned particle.

the complex macropore structure of "real" catalysts and thus the energetics of particle migration are considerably different. Nevertheless, the statistical analyses of PSDs provide useful, though qualitative, guidelines to the relative influences of time, temperature, and atmosphere, in particular enabling comparisons of "oxidising" and "reducing" treatments. Also, it might reasonably be expected that the details of particle morphology revealed by high-resolution observations should also be applicable to the "real" catalyst. Indeed, our comparable studies on real catalysts (*22*) show the same general trends as the models although the magnitude of the effects differ due to different loadings.

Irrespective of the prevailing atmosphere, it appears that higher temperatures generally have considerable influence on

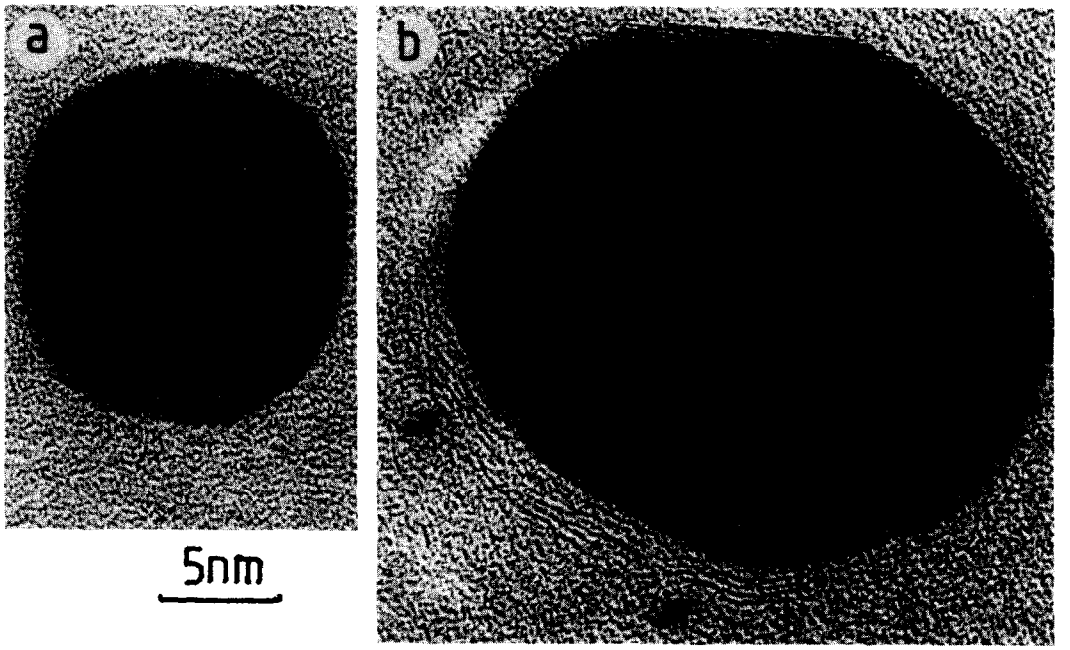

FIG. 8. Model catalyst MC15 after "oxychlorination" at 500°C. (a) Lamellar-twinned Pt particle; (b) poorly crystalline layer (arrowed) partially surrounding particle of Pt.

particle sintering with the exception only of treatment in *pure* reducing environments of catalysts with light metal loadings when sintering was marginal (MC14). It is significant though that the presence of trace impurities, even at the 1-vpm level, is sufficient to alter substantially the sintering characteristics of the model catalyst under such a "reducing" environment. This result thus justifies our insistence on very careful control of the preparation conditions as well as having implications for both previous and future TEM studies involving "real" and model systems. It is also significant that enhanced sintering occurred in the chlorided oxidising atmosphere, thus showing that mechanical re-dispersion of the platinum particles does not take place. (Such treatment is commonly used in the industrial regeneration of platinum catalysts to regain metal surface area (*12*).) Treatment of a "real" reforming catalyst under similar conditions (*16*) also resulted in an enhancement of sintering rates, albeit with much lower platinum loading, confirming that this effect was not an artefact of the model.

The present study has established that the model catalyst particles of platinum are primarily in the crystalline f.c.c. metallic form, with a substantial fraction of these particles (perhaps 30%) containing twin boundaries. Whilst there was no clear evidence for discontinuities or defects at the boundaries which might lead to increased surface area, or special sites for catalytic exchange, it seems possible nevertheless that the atomic arrangements associated with the twinned particles could prove critical to catalytic activity. There were no other obvious changes from bulk f.c.c. structure nor was there any reason to suspect those treated oxidatively at 600°C where some substrate modification around the particles, in the form of a halo, or partial halo, was observed. However, given the treatment temperature of 600°C, no oxide "wetting" of the surface seems likely

and it appears to be most probable that the modified region is associated with some rearrangement of the associated particle induced by particle coalescence (*23*). It is clear from Fig. 8 that the surface "halo" is associated with those parts of the particle where recrystallisation has taken place and well-defined facets have been formed, as distinct from those parts of the particle that retained the profile, or partial profile, of an irregular globule after sintering. A microanalytical study is being undertaken to substantiate the presence, or otherwise, of platinum away from the particles and to investigate further the possible role of the haloes in catalyst regeneration.

ACKNOWLEDGMENTS

The Cambridge University 600-kV high-resolution electron microscope was constructed as a joint project between the Cavendish Laboratory and the Department of Engineering with major financial support from the Science Research Council. We are grateful to the Science Research Council for provision of the JEM 100C at Glasgow and to the Science and Engineering Research Council for continuing support both for the HREM and, in conjunction with ICI Petrochemicals and Plastics Division, Wilton, for the provision of a CASE award for D.W. We would also like to thank Dr. M. Day of ICI Petrochemicals and Plastics Division for his interest and comments on parts of this work.

REFERENCES

1. Flynn, P.C., and Wanke, S. E., *J. Catal.* **37,** 432 (1975).
2. Baker, R. T. K., Thomas, C., and Thomas, R. B., *J. Catal.* **38,** 510 (1975).
3. Ruckenstein, E., and Malhotra, O., *J. Catal.* **41,** 303 (1976).
4. Chu, Y. F., and Ruckenstein, E., *J. Catal.* **55,** 281 (1978).
5. Baker, R. T. K., Prestridge, E. B., and Garten, R. L., *J. Catal.* **56,** 390 (1979).
6. Ruckenstein, E., and Chu, Y. F., *J. Catal.* **59,** 109 (1979).
7. Stulga, J. E., Wynblatt, P., and Tien, J. K., *J. Catal.* **62,** 59 (1980).
8. Baker, R. T. K., *J. Catal.* **63,** 523 (1980).
9. Glassl, H., Kramer, R., and Hayek, K., *J. Catal.* **63,** 167 (1980).
10. Glassl, H., Kramer, R., and Hayek, K., *J. Catal.* **68,** 388 (1981).
11. Johnson, H. F. L., and Keith, C. D., *J. Phys. Chem.* **67,** 200 (1963).
12. Yates, D. J. C., U.S. Patent specification 1,433,864 (1976).
13. Flynn, P. C., and Wanke, S. E., *J. Catal.* **34,** 390 (1974).
14. Yao, H. C., Sieg, M., and Plummer, H. K., *J. Catal.* **59,** 365 (1979).
15. White, D., Baird, T., and Fryer, J. R., *in* "Electron Microscopy 1980" (P. Brederoo and G. Boom, Eds.), Vol. 1, p. 220. Seventh European Regional Conference on Electron Microscopy Foundation, Leiden, 1980.
16. White, D., Baird, T., Fryer, J. R., and Smith, D. J., *in* "Electron Microscopy and Analysis 1981" (M. J. Goringe, Ed.), p. 403. Institute of Physics, Bristol/London, 1982.
17. Flynn, P. C., Wanke, S. E., and Turner, P. S., *J. Catal.* **33,** 233 (1974).
18. Treacy, M. M. H., and Howie, A., *J. Catal.* **63,** 265 (1980).
19. Nixon, W. C., Ahmed, H., Catto, C. J. D., Cleaver, J. R. A., Smith, K. C. A., Timbs, A. E., Turner, P. W., and Ross, P. M., *in* "Developments in Electron Microscopy and Analysis 1977" (D. L. Misell, Ed.), p. 13. Institute of Physics, London, 1978.
20. Cosslett, V. E., *Proc. Roy. Soc. (London) Sect. A* **370,** 1 (1980).
21. Smith, D. J., Camps, R. A., Cosslett, V. E., Freeman, L. A., Saxton, W. O., Nixon, W. C., Ahmed, H., Catto, C. J. D., Cleaver, J. R. A., Smith, K. C. A., and Timbs, A. E. *Ultramicroscopy* **9,** 203 (1982).
22. White, D., Baird, T., Fryer, J. R., Freeman, L. A., Smith, D. J., and Day, M., *J. Catal.* **81,** 119 (1983).
23. Gwathmey, A. T., and Cunningham, R. E., *Advan. Catal.* **10,** 57 (1958).